

pressure ports (18 upper and 17 lower) at the outboard section. Data were recorded at each Mach number and angle-of-attack combination for each model configuration.

### Test Results

The comparative pressure plots made of all model configurations at each Mach number and angle of attack are overlays so nearly identical that any slight difference can be attributed to run repeatability or small differences in Mach number. A pressure plot of the more interesting run comparison is shown in Fig. 3 at Mach number 0.95 for +2-deg angle of attack. In this figure, a comparison overlay is shown which illustrates that, at a Mach number of 0.95 for all slot configurations, all the parameters for each model configuration are nearly identical. Figure 4 is an overlay plot of  $C_L$ ,  $C_D$ , and  $C_M$  vs the angle of attack for all model configurations at 0.95 Mach number. Direct overlays have been made for all the other Mach number conditions with similar results.

### Conclusions

The test results show very conclusively that sectionalized flutter model design is not aerodynamically inaccurate when testing in the transonic speed range. This information can give the flutter engineer confidence that sufficiently accurate data can be obtained from other than a smooth-skin model. It also gives the test engineer a quicker and easier method of testing a larger variety of model parameters early in the aircraft design phase. Sectionalized model tests should be considered as a useful tool for extensive parametric studies at transonic speeds.

### References

- <sup>1</sup>Farmer, M.G. and Hanson, P.H., "Comparison of Supercritical and Conventional Wing Flutter Characteristics," *Proceedings of the AIAA/ASME/SAE 17th Structures, Structural Dynamics and Materials Conference*, King of Prussia, Pa., 1976, pp. 608-614.
- <sup>2</sup>Houwink, R., Kraan, A.N., and Zwaan, R.I., "A Wind-Tunnel Study of the Flutter Characteristics of a Supercritical Wing," *Proceedings of AIAA/ASME/ASCE/AHS 22nd Structures, Structural Dynamics and Materials Conference*, Atlanta, Ga., April 1981, pp. 748-754.
- <sup>3</sup>Grosser, W.F., "A Wind-Tunnel Study of the Aerodynamic Characteristics of a Slotted Versus Smooth-Skin Supercritical Wing," *Proceedings of the AIAA/ASME/ASCE/AHS 23rd Structures, Structural Dynamics and Materials Conference*, New Orleans, La., May 1982, pp. 84-94.

## A New Approach to Optimization for Aerodynamic Applications

Magdi H. Rizk\*

Flow Industries, Inc., Kent, Washington

### Nomenclature

- $E$  = objective function  
 $M$  = Mach number  
 $P$  = vector of design parameters  
 $R$  = residual  
 $x$  = coordinate in the undisturbed flow direction  
 $y$  = vertical coordinate in the upward direction

Received July 6, 1982; revision received Aug. 30, 1982. Copyright © American Institute of Aeronautics and Astronautics, Inc., 1982. All rights reserved.

\*Senior Research Scientist, Research and Technology Division. Member AIAA.

- $\epsilon$  = small positive number determining convergence  
 $\rho$  = density  
 $\phi$  = perturbation velocity potential

### Subscripts and Superscripts

- $c$  = corrected value  
 $F$  = free air condition  
 $R$  = residual  
 $T$  = tunnel condition  
 $\infty$  = undisturbed condition  
 $0$  = minimum value  
 $( )^*$  = optimum value

### Introduction

OPTIMIZATION problems arise in different aerodynamic applications, and their solutions attempt to determine the vector of design parameters,  $P$ , that minimizes the objective function  $E(P; \phi)$ , where  $\phi$  is the solution of the potential flow equation. For example, in airfoil design problems<sup>1</sup>  $P$  contains different shape functions for the airfoil surface, and  $E$  is the drag or negative lift. Wind tunnel wall interference is another example where the above optimization problem arises. There  $P$  may be chosen as a single design parameter (scalar) equal to the freestream Mach number.<sup>2</sup> The objective function  $E$  is chosen to be a measure of the Mach number differences on the model surface in the tunnel and in free air.

The optimization problem under consideration may be stated as follows: Find  $P$  such that

$$\min_P E(P; \phi) \quad (1)$$

with  $\phi$  satisfying the equation

$$\nabla \cdot [\rho \nabla (x + \phi)] = 0$$

or the approximation

$$D(\phi; P) = 0 \quad (2a)$$

subject to the boundary condition

$$B(\phi; P) = 0 \quad (2b)$$

Currently available procedures<sup>1,3</sup> for solving the above minimization problem are time-consuming. Their high cost prevents their regular use in design problems. These procedures are inner-outer iterative procedures. In such procedures, each outer iteration results in a new iterative solution for  $P$  by using an optimization scheme (e.g., the steepest descent method or the conjugate gradient method). However, each outer iteration requires that the objective function be estimated, and, therefore, that a solution for Eq. (2a) be obtained (e.g., by line relaxation) using the new value for  $P$ . Consequently, Eq. (2a) must be solved many times before the optimum  $P$  value is found, resulting in the high cost of calculation.

In this Note, a new and efficient approach to solving problems (1) and (2) is presented. This approach eliminates the need for an inner-outer iterative procedure, and requires that the boundary value problem (2) be solved only once. The approach is tested on a single design parameter problem.

### Formulation

Present procedures for solving problems (1) and (2) use an optimization scheme to determine a sequence of successive approximations,  $P_m$ , where  $m = 1, 2, \dots$ , which converge to the optimum value  $P^*$ . This is the outer iterative process. Within the  $m$ th outer iteration, the boundary value problem (2) is solved by making a number of iterative sweeps (inner iterations). The inner iterative sweeps update the value of  $\phi$ , giving the successively improved approximations  $\phi_m^n$ , where

$n=1,2,\dots$ , which converge to the solution  $\phi_m$ , satisfying the boundary value problem

$$D(\phi_m; \mathbf{P}_m) = 0 \quad m=1,2,\dots$$

$$B(\phi_m; \mathbf{P}_m) = 0 \quad m=1,2,\dots$$

While the standard method of solving problem (2) updates the value of  $\phi$  at the end of each iterative sweep while holding  $\mathbf{P}$  fixed, the new approach presented here updates the value of  $\mathbf{P}$  before each iterative sweep. This results in the successively improved approximations  $(\phi^n, \mathbf{P}^n)$ ,  $n=1,2,\dots$ , which converge to the solution  $(\phi^*, \mathbf{P}^*)$ , satisfying the optimization problems (1) and (2). This basic idea of updating both  $\phi$  and  $\mathbf{P}$  simultaneously can be used to develop a family of efficient optimization schemes. A single parameter scheme belonging to this family is developed and tested here.

The optimization approach is applied to the problem of correcting the freestream Mach number due to wind tunnel wall blockage effects. A similar approach<sup>4</sup> has been applied to the problem of correcting the angle of attack due to wind tunnel wall interference. Combining the present scheme and the scheme of Ref. 4 allows the calculation of Mach number and angle-of-attack corrections.

In the wind tunnel wall interference problem, the design parameter  $\mathbf{P}$  is a scalar equal to the undisturbed free air Mach number  $M_{F\infty}$ . The correction procedure described in Ref. 2 seeks the corrected (optimum) value  $M_{F\infty}^n$  which minimizes the objective function

$$E = \int |M_F - M_T| dS / \int M_T dS \quad (3)$$

where the integrals are taken over the model surface. The objective function here is a measure of the Mach number difference on the model surface in the tunnel and in free air. The flow is assumed to be governed by the transonic small disturbance equation

$$[\rho(I + \phi_x)]_x + \phi_{yy} = 0 \quad (4)$$

where

$$\rho = I - \phi_x + (I - M_\infty^2)\phi_x + [(I - \gamma)/2]\phi_x^2 + \dots$$

Reference 5 describes a procedure for solving the transonic small disturbance equation iteratively by successive line overrelaxation. This procedure is used to solve Eq. (4) with the following modification. In a standard solution of Eq. (4), the potential function  $\phi$  is updated at the end of each iterative sweep with the iterative solution  $\phi^{n+1}$  resulting at the end of the  $n+1$  iterative sweep. Throughout this process, the value of  $M_{F\infty}$  is held fixed. In the current optimization procedure, the value of  $M_{F\infty}$  is updated before each relaxation sweep.

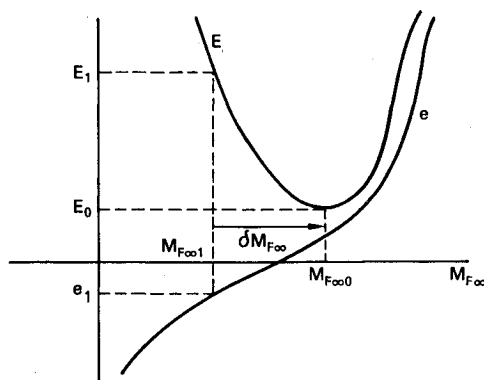


Fig. 1 Sketch showing the relation between  $E$  vs  $M_{F\infty}$  and  $e$  vs  $M_{F\infty}$ .

Figure 1 shows sketches for the functions  $E(M_{F\infty})$  and  $e(M_{F\infty})$  where

$$e(M_{F\infty}) \equiv \int (M_F - M_T) dS / \int M_T dS$$

From the figure, it is noted that for a given value of  $M_{F\infty}$  ( $=M_{F\infty l}$ ), an incremental value  $\delta M_{F\infty}$  may be found to produce a new value for  $M_{F\infty}$  ( $=M_{F\infty 0} = M_{F\infty l} + \delta M_{F\infty}$ ) corresponding to the minimum value of  $E$  ( $=E_0$ ). The value of  $\delta M_{F\infty}$  is positive (or negative) if the value of  $(dE_1/dM_{F\infty})$  ( $(de_1/dM_{F\infty})$ ) is negative (or positive). These observations lead to the following scheme for updating the freestream Mach number before the  $n+1$  relaxation sweep.

$$M_{F\infty}^{n+1} = M_{F\infty}^n + \delta M_{F\infty}^{n+1}$$

where

$$\delta M_{F\infty}^{n+1} = 1/2 \delta M_{F\infty}^n [c_1 (s^n + 1) + c_2 (s^n - 1)] \quad (5)$$

$$s^n = - \frac{F^n \delta M_{F\infty}^n}{|F^n \delta M_{F\infty}^n|}$$

$$F^n = (E^n - E^{n-1}) (e^n - e^{n-1})$$

$$E^n = E(M_{F\infty}^n; \phi^n) \quad e^n = e(M_{F\infty}^n; \phi^n)$$

and  $c_1, c_2$  are constants with  $c_1 > 1, c_2 < 1$ . The iterative process continues until the convergence criterion

$$\max(|R^n| - \epsilon_R, |\delta M_{F\infty}^n| - \epsilon_M) < 0$$

is met, where  $R^n$  is the maximum residual for the set of finite-difference equations at the  $n$ th iteration, and  $\epsilon_R$  and  $\epsilon_M$  are small positive numbers. Equation (5) determines the sign and the magnitude of the incremental value  $\delta M_{F\infty}^{n+1}$ . The sign of the incremental value is determined here in a similar manner to that in Ref. 2. However, the magnitude is determined in a manner suggested by W.B. Kemp Jr. during a recent visit to NASA Langley Research Center. The scheme used in determining the magnitude of  $\delta M_{F\infty}^{n+1}$  in Ref. 2 proved to be unreliable.

## Results and Discussion

Mach number corrections are calculated for a NACA 0012 airfoil of chord 1.0 and zero angle of attack located in the middle of a solid-wall wind tunnel of height 3.26 chord

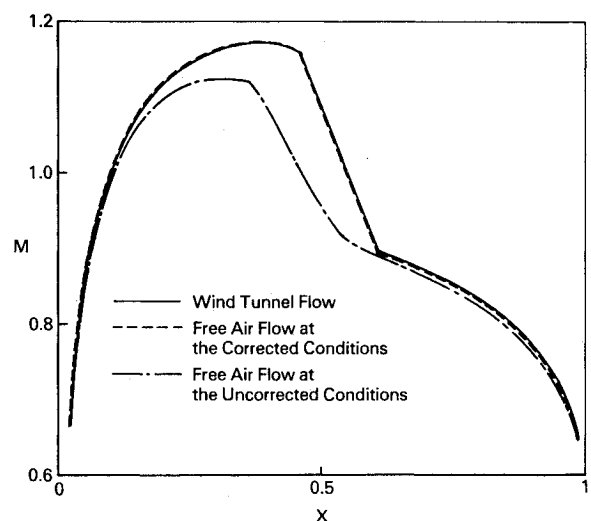


Fig. 2 Mach number distribution on airfoil surface.

**Table 1** Number of iterations

	Coarse mesh	Fine mesh
Present calculation	116	189
Standard calculation	132	176

lengths. The wind tunnel freestream Mach number is taken to be 0.8.

A comparison between the Mach number distribution on the airfoil surface for the wind tunnel flow ( $M_\infty = 0.8$ ), the free airflow at the corrected condition ( $M_\infty = 0.8169$ ), and the free airflow at the uncorrected condition ( $M_\infty = 0.8$ ) is given in Fig. 2. The objective function was reduced from the value  $E = 0.036$  for the flow with the uncorrected Mach number ( $M_\infty = 0.8$ ) to the value  $E = 0.003$  for the flow with the corrected Mach number ( $M_\infty = 0.8169$ ).

To estimate the effect of correcting the Mach number, as described above, on the rate of convergence of the flowfield solution, a standard calculation with  $M_{F\infty} = 0.8169$  was performed. In this calculation,  $M_{F\infty}$  was not updated during the iterative process. A solution obtained on a coarse computational mesh was used as an initial guess for solving the problem on the final mesh. A comparison between the number of iterations required for the convergence ( $\epsilon_R = 0.0005$ ,  $\epsilon_M = 0.00005$ ) of the present iterative process, and the number of iterations required for the convergence ( $\epsilon_R = 0.0005$ ) of the standard iterative process is given in Table 1. The table indicates comparable convergence properties for the present iterative process, and the standard iterative process.

In the above calculations, the initial guess for the value of  $M_{F\infty}^c$  was taken to be 0.83. The initial incremental value  $\delta M_F^c$  and the constants  $c_1$  and  $c_2$  were set equal to 0.002, 1.2, and

0.6, respectively. No attempt has been made to optimize the values of these parameters in the present calculations.

### Concluding Remarks

A new approach to solving optimization problems that involve nonlinear partial differential equations is presented. This approach eliminates the need for an inner-outer iterative procedure. It solves the partial differential equation only once, thereby reducing the cost of computation to an extent which would allow its use as a practical tool in optimization problems. The new approach has been tested here on a single design parameter problem through the use of a specially developed scheme. The ideas presented here, however, are applicable to multidesign parameter problems.

### Acknowledgment

This work was sponsored by NASA Langley under Contract NAS1-16262.

### References

- <sup>1</sup>Vanderplaats, G.N., "An Efficient Algorithm for Numerical Airfoil Optimization," *Journal of Aircraft*, Vol. 16, Dec. 1979, pp. 842-847.
- <sup>2</sup>Rizk, M.H., Hafez, M., Murman, E.M., and Lovell, D., "Transonic Wind Tunnel Wall Interference Corrections for Three-Dimensional Models," AIAA Paper 82-0588, March 1982.
- <sup>3</sup>Hicks, R.M., Murman, E.M., and Vanderplaats, G.N., "An Assessment of Airfoil Design by Numerical Optimization," NASA TM X-3092, July 1974.
- <sup>4</sup>Rizk, M.H., "A New Optimization Technique Applied to Wind Tunnel Angle-of-Attack Corrections," Note 198, Flow Research Company, Kent, Wash., Feb. 1982.
- <sup>5</sup>Rizk, M.H., "Propeller Slipstream/Wing Interaction in the Transonic Regime," *Journal of Aircraft*, Vol. 18, March 1981, pp. 184-191.

### AIAA Meetings of Interest to Journal Readers\*

Date	Meeting (Issue of AIAA Bulletin in which program will appear)	Location	Call for Papers†	Abstract Deadline
<b>1983</b>				
Jan. 10-13	AIAA 21st Aerospace Sciences Meeting and Technical Display (Nov.)	MGM Grand Hotel Reno, Nev.	April 82	July 6, 82
April 11-13	AIAA 8th Aeroacoustics Conference (Feb.)	Terrace Garden Inn Atlanta, Ga.	July/ Aug. 82	Oct. 1, 82
May 2-4	24th AIAA/ASME/ASCE/AHS Structures, Structural Dynamics, and Materials Conference (March)	Sahara Hotel Lake Tahoe, Nev.	June 82	Aug. 31, 82
May 10-12	AIAA Annual Meeting and Technical Display	Long Beach Convention Center, Long Beach, Calif.		
June 1-3	AIAA/ASCE/TRB/ATRIF/CASI International Air Transportation Conference (April)	The Queen Elizabeth Hotel Montreal, Quebec, Canada	Oct. 82	Invited
June 6-11‡	6th International Symposium on Air Breathing Engines	Paris, France	April 82	June 1, 82
June 13-15	AIAA Flight Simulation Technologies Conference (April)	Niagara Hilton Niagara Falls, N.Y.	Sept. 82	Dec. 1, 82
June 27-29	AIAA/SAE/ASME 19th Joint Propulsion Conference and Technical Display (April)	Westin Hotel Seattle, Wash.	Sept. 82	Dec. 7, 82
July 13-15	AIAA Applied Aerodynamics Conference (May)	Radisson Ferncroft Hotel and Country Club Danvers, Mass.	Oct. 82	Jan. 3, 82

\*For a complete listing of AIAA meetings, see the current issue of the AIAA Bulletin.

†Issue of AIAA Bulletin in which Call for Papers appeared.

‡Meetings cosponsored by AIAA.